

Lipophilicity of Aminopyridazinone Regioisomers

MASSUD A. S. ANWAIR,[§] LÁSZLÓ KÁROLYHÁZY,[§] DIÁNA SZABÓ,[§]
 BALÁZS BALOGH,[§] ISTVÁN KÖVESDI,[†] VERONIKA HARMAT,[‡] JUDIT KRENYÁ CZ,[‡]
 ÁKOS GELLÉRT,[‡] KRISZTINA TAKÁCS-NOVÁK,^{*#} AND PÉTER MÁTYUS^{*§}

Departments of Organic Chemistry and Pharmaceutical Chemistry, Semmelweis University,
 Hógyes E. u. 7–9, 1092 Budapest, Hungary; Vichem Chemie Ltd., Hermann O. u. 15,
 1022 Budapest, Hungary; and Department of Theoretical Chemistry, Eötvös Loránd University,
 Pázmány Péter sétány 1, 1117 Budapest, Hungary

Ten pairs of pyridazinone regioisomers were prepared, and their lipophilicity was described by the logarithm of the octanol/water partition coefficient ($\log P$) determined experimentally and calculated with prediction methods. The 4- and 5-(substituted amino)-3(2*H*)-pyridazinone regioisomers were synthesized by nucleophilic substitution of one of the chloro atoms of 4,5-dichloro-2-methyl-3(2*H*)-pyridazinone or its 6-nitro derivative. Structures of new compounds were proven by spectroscopic methods. The experimental $\log P$ values were obtained by a shake flask method in octanol and a Sørensen buffer (pH 7.4) solvent system. A consequent difference was found in the lipophilicity of regioisomers. For each isomer pair, the $\log P$ value of the 4-isomer was significantly (average by 0.75 \log unit) higher than that of the 5-isomer. Some quantum chemical calculations as well as X-ray analysis of two pairs of regioisomers were also carried out to gain insight into the structural differences of regioisomers. The $\log P$ values were calculated by the fragmental approach KOWWIN and a QSPR analysis (3DNET). The a priori KOWWIN gave poor agreement, but with the programs KOWWIN with EVA (experimental value adjusted) and 3DNET, the results were generally in agreement with experiment.

KEYWORDS: Aminopyridazinone regioisomers; nucleophilic substitution; octanol/water partitioning; $\log P$; $\log P$ calculators; X-ray

INTRODUCTION

3(2*H*)-Pyridazinones substituted with an amino group at the 5-position represent an important and thoroughly investigated class of pesticides. Some representatives of this class of compounds have been marketed and used in practice (1).

We have also discovered several aminopyridazinones with remarkable biological activities; for example, antiarrhythmic (2), nootropic (memory-improving) (3), and, more recently, anti-fungal (4) effects have been observed. The most active compounds of the antifungal series of pyridazinones were found to exhibit antagonistic effects against a broad spectrum of pathogenic fungi including *Saccharomyces cerevisiae*. Most probably, the antifungal activity of these compounds is related to the inhibitory action against β 1,3-glucan synthase and chitin synthase enzymes that catalyze the synthesis of the major polymers of the fungal cell wall. Further in vitro and in vivo studies are now in progress to exploit these valuable properties;

the agricultural and sanitation fields have been primarily considered for application.

Interestingly, in almost all of the above series of pyridazinones, significant differences in the biological activities of regioisomeric 4- and 5-amino compounds have been detected. For these different biological activities, the difference in hydrophobicity of the regioisomers may be expected to be at least partially responsible. Therefore, we thought that a comparison of the logarithm of the octanol/water partition coefficients (i.e., $\log P$ values) of the regioisomers might provide useful information. Indeed, our preliminary study on two pairs of regioisomers (2c,g and 3c,g, Scheme 1) revealed that $\log P$ values of the 4-amino isomers were significantly higher (5), supporting the idea that there might be some correlation between the antifungal activity and $\log P$ of regioisomers.

The literature showed that, apart from our preliminary work and the excellent well-known study of Testa et al. on the influence of stereochemical factors on the $\log P$ of diastereomers, no relevant study has been done on the lipophilicity of regioisomers (6). Testa et al. found that some pairs of diastereomers showed the same lipophilicity, whereas others displayed differences of up to 1 \log unit. For rigid compounds with one polar group, differences in lipophilicity were related to differences in solvent accessible surface area. For flexible compounds

* Corresponding authors [(P.M.) fax/telephone +36-1-217-0851, e-mail matypet@szerves.sote.hu; (K.T.-N.) fax +36-1-2170890, telephone +36-1-2155241, e-mail novkri@hogyes.sote.hu.

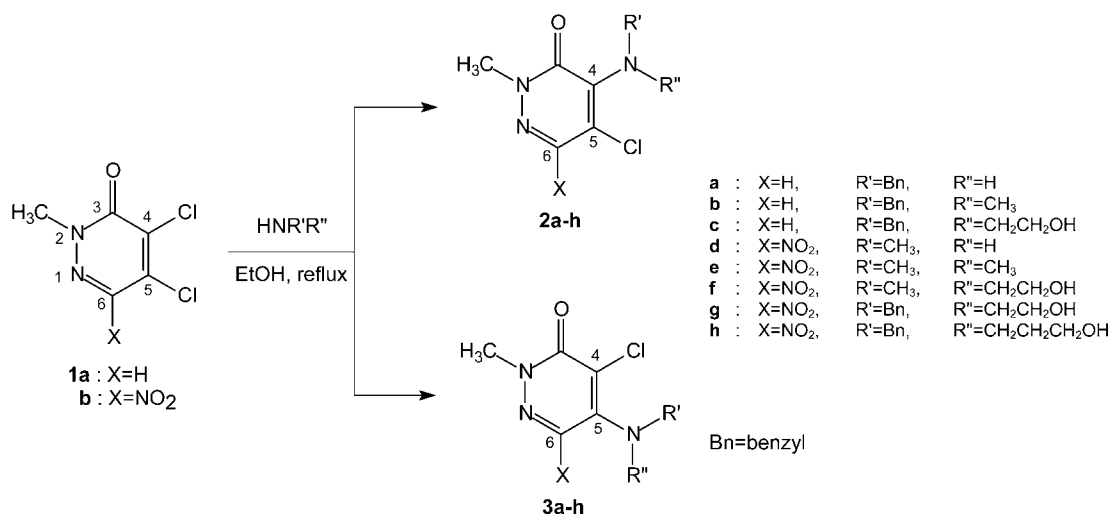
[†] Vichem Chemie Ltd.

[‡] Eötvös Loránd University.

[§] Department of Organic Chemistry, Semmelweis University.

[#] Department of Pharmaceutical Chemistry, Semmelweis University.

Scheme 1



or for compounds with more polar groups, the structural effects appeared to be quite complex.

The log *P* values can also be estimated by calculations (7–10). Computation of log *P* has nowadays an increasing importance in drug discovery. Unfortunately, the methods available have not proven to be uniformly reliable. For instance, in the case of a diverse set of 9392 compounds, the log *P* values were calculated according to 13 methods and compared to the experimental values. The absolute deviations between observed and calculated values varied from 0.36 to 0.98 on average, much higher than the acceptable ± 0.4 log range (11). Our other experiences with six log *P* calculators were also quite disappointing when we tested their performances on two pairs of pyridazinone regioisomers (**2c,g** and **3c,g**, Scheme 1). There were only two methods, the fragmental-based KOWWIN with EVA (experimental value adjusted) option and the 3DNET analysis, which reproduced at least the trend of experimental lipophilicity of the isomers.

As an extension of this work, we now report on the synthesis and experimental log *P* determination of 10 pairs of aminopyridazinones containing various bulky substituents either at position 4 or at position 5 to confirm the tendency observed previously for the difference of lipophilicity of 4- and 5-aminopyridazinone regioisomers. We also thought that in this way we could get a closer insight into the important effects of structural features on lipophilicity. We report the results of calculations obtained by KOWWIN and 3DNET in order to illustrate their reliability.

MATERIALS AND METHODS

All melting points were determined on a Büchi 530 melting point apparatus and are uncorrected; the values are given in degrees centigrade. The IR spectra were recorded on a Perkin-Elmer 1600 FTIR instrument in potassium bromide pellets. The ¹H NMR spectra were recorded at room temperature in the solvent indicated, using the ²H signal of the solvent as the lock and tetramethylsilane as the internal standard. Chemical shifts are given in parts per million. Bruker AM at 200 MHz was used. The assignments of ¹³C NMR spectra were supported by DEPT-135 spectra. Coupling constants (*J*) are given in hertz. For log *P* determinations, The concentration of the compounds was determined spectrophotometrically on a Hewlett-Packard 8452A spectrophotometer. The shake flask method was carried out as described previously (12–14). The elementary analyses were performed on a Carlo Erba model 1012 elemental analyzer. For column chromatography, Kieselgel 60 (Aldrich, 0.063–0.2 mm silica gel) was used; TLC analysis utilized silica gel 60 F₂₅₄ (Merck) plates. Solvent mixtures

used for chromatography are always given in a volume/volume ratio. Solvents were purified by distillation and/or standard procedures. All reagents were purchased from Aldrich (Sigma-Aldrich Kft) and used as received. Octanol used for the shake flask method was purchased also from Aldrich (HPLC grade).

4,5-Dichloro-2-methyl-3(2*H*)-pyridazinone (**1a**) and 4,5-dichloro-2-methyl-6-nitro-3(2*H*)-pyridazinone (**1b**) were synthesized according to known procedures (15, 16). The 4- or 5-chloro atom of compound **1a,b** could easily be substituted by an amino group (cf. refs 17 and 18). Compounds **2a–h** and **3a–h** (Scheme 1) were prepared in this way by nucleophilic substitution reactions of compounds **1a** and **1b** with methylamine, dimethylamine, benzylamine, *N*-methylbenzylamine, *N*-benzylaminoethanol, and *N*-benzylaminopropanol as described below. Of these compounds **2a,b** and **3a,b** (17), **2g,h** and **3g,h** (18), and **3f** (19) were already described.

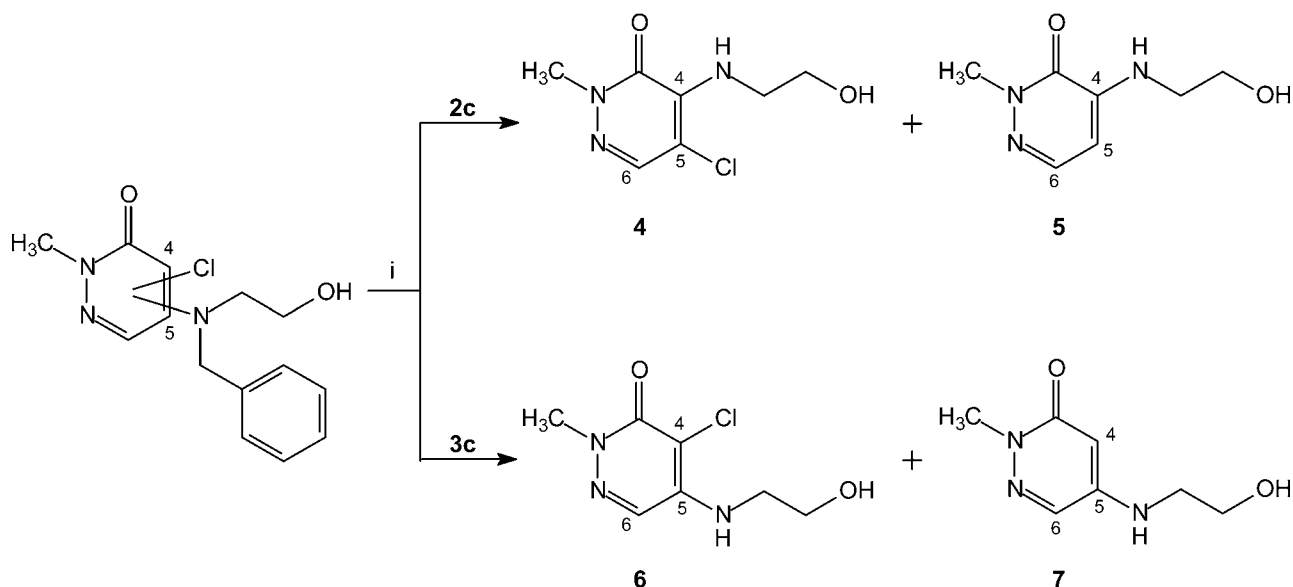
When compound **2c** or **3c** was refluxed in ethanol in the presence of cyclohexene and palladium on carbon catalyst, besides the debenzylated chloro derivatives **4** (34%) or **6** (68%), respectively, the dehalogenated compounds **5** (4%) or **7** (27%) were also formed, and they could be isolated as minor products (Scheme 2).

Preparation of Compounds. General Procedure for Preparation of *N*-Benzylamino Derivatives 2a–c, 2g,h, 3a–c, and 3g,h (Scheme 1). To a solution of 4,5-dichloro-2-methyl-3(2*H*)-pyridazinone (**1a**) or 4,5-dichloro-2-methyl-6-nitro-3(2*H*)-pyridazinone (**1b**) (15 mM) in dry ethanol (60 mL) was added the appropriate amino compound (45–60 mM), and the mixture was heated under reflux for 3–8 h (monitored by TLC). The reaction mixture was evaporated to dryness in vacuo. Then water was added to the residue, and the mixture was acidified with aqueous 2 M hydrochloric acid. The solution was extracted with ethyl acetate, and the combined organic phase was dried over anhydrous magnesium sulfate. The solvent was evaporated in vacuo, and the 4- and 5-benzylamino regioisomers were separated by crystallization (cryst) and/or column chromatography (col chrom) in pure forms.

Compounds **2a** (mp 97–98 °C), **3a** (mp 184–185 °C), **2b** (oil), and **3b** (oil) have already been reported; for spectroscopic data, see ref 17.

Compound **2c**: white crystals (col chrom, chloroform/ethyl acetate 1:1; *R_f* = 0.38; yield = 16%); mp 82–83 °C; IR (ν) 3442, 2903, 1639, 1570, 1522, 1447, 1403, 1352, 1314, 1227, 1147, 1048, 935 cm⁻¹; ¹H NMR (deuteriochloroform) δ 3.43 (t, 2H, OCH₂, *J* = 4.8 Hz), 3.66 (t, 2H, NCH₂), 3.74 (s, 3H, NCH₃), 4.56 (s, 2H, benzyl CH₂), 7.22–7.28 (m, 5H, benzyl aromatic protons), 7.65 (s, 1H, 6-H); ¹³C NMR (deuteriochloroform) δ 40.4 (NCH₃), 53.6 (NCH₂), 54.3 (benzyl CH₂), 59.5 (OCH₂), 127.4 (C-4'), 128.0 (C-2', C-6'), 128.4 (C-5), 128.5 (C-3', C-5'), 137.9 (C-1'), 138.1 (C-6), 144.8 (C-4), 160.9 (C-3). Anal. Calcd for C₁₄H₁₆ClN₃O₂: C, 57.24; H, 5.49; N, 14.34. Found: C, 57.15, H, 5.52, N, 14.22.

Compound **3c**: white crystals (cryst, ethyl acetate, *R_f* = 0.14 chloroform/ethyl acetate 1:1; yield = 20%); mp 121 °C; IR (ν) 3427, 2927, 1625, 1496, 1329, 1141, 1049, 728 cm⁻¹; ¹H NMR (deuterio-

Scheme 2^a

^a Reaction conditions: (i) Pd/C, cyclohexane, EtOH, reflux.

chloroform) δ 3.46 (s, 1H, OH), 3.61 (t, 2H, NCH_2 , $J = 5.4$ Hz), 3.66 (s, 3H, NCH_3), 3.84 (t, 2H, OCH_2), 4.73 (s, 2H, benzyl CH_2), 7.21–7.33 (m, 5H, benzyl aromatic protons), 7.72 (s, 1H, 6-H); ¹³C NMR (deuteriochloroform) δ 40.3 (NCH_3), 52.9 (NCH_2), 55.0 (benzyl CH_2), 60.4 (OCH_2), 114.7 (C-4), 127.2 (C-2', C-6'), 127.6 (C-4'), 128.8 (C-3', C-5'), 131.8 (C-6), 136.7 (C-1'), 147.7 (C-5), 158.8 (C-3). Anal. Calcd for $\text{C}_{14}\text{H}_{16}\text{ClN}_3\text{O}_2$: C, 57.24; H, 5.49; N, 14.34. Found: C, 57.25, H, 5.45, N, 14.36.

Compounds **2g** (oil), **3g** (mp 139–140 °C), **2h** (oil), and **3h** (mp 75–76 °C) have already been reported; for spectroscopic data, see ref 18.

General Procedure for Preparation of 4- and 5-N-Methylamino and 4- and 5-N,N-Dimethylamino Derivatives 2d,e and 3d,e (Scheme 1). 4,5-Dichloro-2-methyl-6-nitro-3(2H)-pyridazinone (**1b**) (4.5 mM) was dissolved in 33% alcoholic methylamine solution or in 25% alcoholic dimethylamine solution (30 mL), respectively, and the solution was stirred for 18 h at room temperature. The reaction mixture was evaporated to dryness in vacuo. The 4- and 5-amino regioisomers thus formed were separated by column chromatography using chloroform as eluent to give the regioisomers in pure forms.

Compound **2d**: yellow crystals ($R_f = 0.63$ toluene/methanol 8:2; yield = 26%); mp 175–176 °C; IR (ν) 3500, 3286, 2926, 1639, 1607, 1550, 1497, 1345 cm^{-1} ; ¹H NMR (deuteriochloroform) δ 3.44 (d, 3H, NHCH_3 , $J = 5.8$ Hz), 3.74 (s, 3H, NCH_3), 6.42 (d, 1H, NH); ¹³C NMR (deuteriochloroform) δ 31.9 (NHCH_3), 40.2 (NCH_3), 96.3 (C-4), 142.2 (C-5, C-6), 155.3 (C-3). Anal. Calcd for $\text{C}_6\text{H}_7\text{ClN}_4\text{O}_3$: C, 32.96; H, 3.23; N, 25.63. Found: C, 33.24, H, 3.23, N, 25.52.

Compound **3d**: yellow crystals ($R_f = 0.38$ toluene/methanol 8:2; yield = 7%); mp 189–190 °C; IR (ν) 3500, 3308, 2924, 1648, 1602, 1542, 1463, 1398, 1285 cm^{-1} ; ¹H NMR (deuteriochloroform) δ 3.28 (d, 3H, NHCH_3 , $J = 5.6$ Hz), 3.84 (s, 3H, NCH_3), 6.62 (d, 1H, NH); ¹³C NMR (deuteriochloroform) δ 32.8 (NHCH_3), 41.3 (NCH_3), 109.9 (C-4), 140.8 (C-5, C-6), 158.1 (C-3). Anal. Calcd for $\text{C}_6\text{H}_7\text{ClN}_4\text{O}_3$: C, 32.96; H, 3.23; N, 25.63. Found: C, 33.05, H, 3.31, N, 25.67.

Compound **2e**: yellow crystals ($R_f = 0.77$ toluene/methanol 8:2; yield = 41%); mp 71–72 °C; IR (ν) 3424, 2924, 1656, 1536, 1429, 1365 cm^{-1} ; ¹H NMR (deuteriochloroform) δ 3.24 [s, 6H, $\text{N}(\text{CH}_3)_2$], 3.71 (s, 3H, NCH_3); ¹³C NMR (deuteriochloroform) δ 40.3 (NCH_3), 43.0 [$\text{N}(\text{CH}_3)_2$], 107.1 (C-4), 146.4 (C-5, C-6), 157.7 (C-3). Anal. Calcd for $\text{C}_7\text{H}_9\text{ClN}_4\text{O}_3$: C, 36.14; H, 3.89; N, 24.09. Found: C, 36.33, H, 3.97, N, 24.51.

Compound **3e**: yellow crystals ($R_f = 0.63$ toluene/methanol 8:2; yield = 29%); mp 109–110 °C; IR (ν) 3500, 2926, 1656, 1593, 1541, 1509, 1392 cm^{-1} ; ¹H NMR (deuteriochloroform) δ 2.96 [s, 6H, $\text{N}(\text{CH}_3)_2$], 3.79 (s, 3H, NCH_3); ¹³C NMR (deuteriochloroform) δ 40.65

(NHCH_3), 41.7 [$\text{N}(\text{CH}_3)_2$], 122.7 (C-4), 143.0 and 145.1 (C-5, C-6), 158.3 (C-3). Anal. Calcd for $\text{C}_7\text{H}_9\text{ClN}_4\text{O}_3$: C, 36.14; H, 3.89; N, 24.09. Found: C, 36.23, H, 4.01, N, 24.14.

Preparation of 4- and 5-N-2-Hydroxyethyl-N-methylamino Derivatives (2f and 3f) (Scheme 1) (19). To an ice-cooled solution of 4,5-dichloro-2-methyl-6-nitro-3(2H)-pyridazinone (**1b**) (4.5 mM) in dry ethanol (20 mL) was added dropwise 2-(N-methylamino)ethanol (13.3 mM). The reaction mixture was allowed to warm to room temperature and was stirred at room temperature for 2 h. The solvent was evaporated in vacuo. The residue was taken up in water (20 mL), and the solution was acidified with aqueous 2 M hydrochloric acid and extracted with chloroform (3 \times 20 mL). The combined organic phase was dried over anhydrous magnesium sulfate. The solvent was evaporated in vacuo, and the 4- and 5-regioisomers thus formed were separated by column chromatography with a 1:16 mixture of ethyl acetate/chloroform as eluent to give the regioisomers in pure forms.

Compound **2f**: yellow oil ($R_f = 0.15$ ethyl acetate/chloroform 1:16; yield = 26%); IR (ν) 3422, 2923, 1651, 1539, 1426, 1363, 1276, 1213, 1076, 1019 cm^{-1} ; ¹H NMR (deuteriochloroform) δ 3.19 [s, 3H, $\text{N}(\text{CH}_3)_2$], 3.47 (t, 1H, OH), 3.69 (t, 2H, NCH_2 , $J = 5.4$ Hz), 3.74 (s, 3H, NCH_3), 3.84 (t, 2H, OCH_2); ¹³C NMR (deuteriochloroform) δ 40.1 and 40.8 (2 \times NCH_3), 54.6 (NCH_2), 59.1 (OCH_2), 110.9 (C-4), 147.1 (C-5), 149.3 (C-6), 158.6 (C-3). Anal. Calcd for $\text{C}_8\text{H}_{11}\text{ClN}_4\text{O}_4$: C, 36.58; H, 4.22; N, 21.33. Found: C, 36.79; H, 4.24; N, 21.73.

Compound **3f** (mp 98–99 °C) was already reported; for spectroscopic data, see ref 19.

General Procedure for Preparation of Compounds 4–7 (Scheme 2). To a solution of 4- or 5-N-benzyl-N-2-hydroxyethylamino derivative (**2c** and **3c**) (3.4 mM) in dry ethanol (30 mL) were added 10% Pd/C catalyst (0.3 g) and cyclohexene (3 mL). The suspension was heated under reflux for 2 h. The reaction mixture was filtered, and the filtrate was evaporated in vacuo. The white crude product was purified by column chromatography using a 4:1 mixture of toluene/methanol as eluent to give two products, **4** and **5** starting from **2c** and **6** and **7** starting from **3c**.

Compound **4**: white crystals ($R_f = 0.48$ toluene/methanol 8:2; yield = 68%); mp 70–71 °C; IR (ν) 3360, 2886, 1618, 1541, 1458, 1411, 1351, 1261, 1132, 1043 cm^{-1} ; ¹H NMR (deuteriochloroform) δ 3.25 (t, 1H, OH, $J = 5.2$ Hz), 3.71 (s, 3H, NCH_3), 3.78–3.96 (m, 4H, NCH_2 and OCH_2), 6.22 (s, 1H, NH), 7.50 (s, 1H, 6-H); ¹³C NMR (deuteriochloroform) δ 40.2 (NCH_3), 46.1 (NCH_2), 62.1 (OCH_2), 107.2 (C-5), 139.5 (C-6), 139.8 (C-4), 156.6 (C-3). Anal. Calcd for $\text{C}_7\text{H}_{10}\text{ClN}_3\text{O}_2$: C, 41.29; H, 4.95; N, 20.64. Found: C, 41.23; H, 4.97; N, 20.55.

Compound **5**: white crystals ($R_f = 0.35$ toluene/methanol 8:2; yield = 4%); mp 68–69 °C; IR (ν) 3386, 2946, 1599, 1557, 1497, 1452,

1373, 1234, 1065, 882 cm^{-1} ; $^1\text{H NMR}$ (deuteriochloroform) δ 3.32 (q, 2H, NCH_2 , $J = 5.6$ Hz), 3.76 (s, 3H, NCH_3), 3.80–4.00 (m, 3H, OH and OCH_2), 6.02 (d, 1H, 5-H), 6.53 (s, 1H, NH), 7.58 (d, 1H, 6-H, $J = 5.2$ Hz); $^{13}\text{C NMR}$ (deuteriochloroform) δ 40.2 (NCH_3), 45.3 (NCH_2), 60.2 (OCH_2), 97.6 (C-5), 138.8 (C-6), 144.2 (C-4), 157.1 (C-3). Anal. Calcd for $\text{C}_7\text{H}_{11}\text{N}_3\text{O}_2$: C, 49.70; H, 6.55; N, 24.84. Found: C, 49.64; H, 6.39; N, 24.84.

Compound **6**: white crystals ($R_f = 0.16$ toluene/methanol 8:2; yield = 34%); mp 133–134 $^\circ\text{C}$; IR (ν) 3284, 2926, 1611, 1522, 1445, 1402, 1317, 1270, 1062 cm^{-1} ; $^1\text{H NMR}$ (deuteriochloroform) δ 3.39 (t, 2H, NCH_2), 3.51 (qua, 2H, OCH_2), 3.57 (s, 3H, NCH_3), 4.86 (t, 1H OH, $J = 5.4$ Hz), 6.49 (s, 1H, NH, $J = 6.2$ Hz), 7.87 (s, 1H, 6-H); $^{13}\text{C NMR}$ (deuteriochloroform) δ 39.5 (NCH_3), 44.5 (NCH_2), 60.5 (OCH_2), 104.2 (C-4), 126.7 (C-6), 144.9 (C-5), 156.7 (C-3). Anal. Calcd for $\text{C}_7\text{H}_{10}\text{ClN}_3\text{O}_2$: C, 41.29; H, 4.95; N, 20.64. Found: C, 41.05; H, 4.92; N, 20.42.

Compound **7**: white crystals ($R_f = 0.12$ toluene/methanol 8:2; yield = 27%); mp 143–144 $^\circ\text{C}$; IR (ν) 3252, 2935, 1630, 1535, 1459, 1335, 1289, 1073 cm^{-1} ; $^1\text{H NMR}$ (deuteriochloroform) δ 3.05 (qa, 2H, NCH_2), 3.52 (qua, 2H, OCH_2), 3.45 (s, 3H, NCH_3), 4.81 (t, 1H OH, $J = 5.4$ Hz), 5.48 (d, 1H, 4-H), 6.94 (t, 1H, NH, $J = 5.2$ Hz), 7.49 (d, 1H, 6-H, $J = 6.2$ Hz); $^{13}\text{C NMR}$ (deuteriochloroform) δ 38.1 (NCH_3), 44.4 (NCH_2), 58.7 (OCH_2), 94.0 (C-4), 130.8 (C-6), 149.2 (C-5), 160.9 (C-3). Anal. Calcd for $\text{C}_7\text{H}_{11}\text{N}_3\text{O}_2$: C, 49.70; H, 6.55; N, 24.84. Found: C, 49.20; H, 6.52; N, 24.74.

Crystal Structures of 2c, 3c and 2e, 3e. Single crystals of **2c**, **3c** and **2e**, **3e** were mounted on glass fibers and transferred to the diffractometer (Rigaku RAXIS-IIc imaging plate detector, Rigaku RU-200HB X-ray generator, graphite monochromated Mo $\text{K}\alpha$ radiation) for data collection. All data were collected at 293 K. Crystal data are shown below with estimated standard deviation in the final digits in parentheses. **2c**: $\text{C}_{14}\text{H}_{16}\text{ClN}_3\text{O}_2$, $M = 293.75$, orthorhombic, space group Pbcn, $a = 1.6195(6)$ nm, $b = 0.7074(3)$ nm, $c = 2.4167(8)$ nm, $V = 2.769(2)$ nm^3 , $Z = 8$, $D_c = 1.409$ g cm^{-3} , μ (Mo– $\text{K}\alpha$) = 0.281 mm^{-1} , 1756 unique reflections. **3c**: $\text{C}_{14}\text{H}_{16}\text{ClN}_3\text{O}_2$, $M = 293.75$, triclinic, space group P-1, $a = 0.9082(3)$ nm, $b = 0.9577(9)$ nm, $c = 0.8994(9)$ nm, $\alpha = 116.98(4)^\circ$, $\beta = 99.98(9)^\circ$, $\gamma = 82.47(9)^\circ$, $V = 0.685(1)$ nm^3 , $Z = 2$, $D_c = 1.414$ g cm^{-3} , μ (Mo– $\text{K}\alpha$) = 0.284 mm^{-1} , 1295 unique reflections. **2e**: $\text{C}_7\text{H}_9\text{ClN}_4\text{O}_3$, $M = 232.63$, monoclinic, space group Pc, $a = 0.4027(5)$ nm, $b = 0.879(1)$ nm, $c = 1.386(2)$ nm, $\beta = 95.8(1)^\circ$, $V = 0.488(1)$ nm^3 , $Z = 2$, $D_c = 1.583$ g cm^{-3} , μ (Mo– $\text{K}\alpha$) = 0.385 mm^{-1} , 1045 unique reflections. **3e**: $\text{C}_7\text{H}_9\text{ClN}_4\text{O}_3$, $M = 232.63$, monoclinic, space group C2/c, $a = 1.139(7)$ nm, $b = 0.994(6)$ nm, $c = 1.717(3)$ nm, $\beta = 97.4(4)^\circ$, $V = 1.93(2)$ nm^3 , $Z = 8$, $D_c = 1.602$ g cm^{-3} , μ (Mo– $\text{K}\alpha$) = 0.390 mm^{-1} , 1986 unique reflections. For all data sets data processing was carried out using the software supplied with the diffractometer. Structure solutions with direct methods were carried out with the teXsan Crystal Structure Analysis Package (Molecular Structure Co., Houston, TX, 1992). The refinements were carried out using the SHELXL-93 program (Sheldrick, G. M. University of Göttingen, Germany, 1993) with full matrix least-squares method on F^2 . All non-hydrogen atoms were refined anisotropically. Hydrogen atoms were generated on the basis of geometric evidence, and their positions were refined by the riding model. Hydrogen atoms of the OH groups were generated to form the best hydrogen bonds. For **2c** two disordered OH hydrogen atoms were generated with occupancies of 0.5. Final R indices for **2c** are $R = 0.1001$ and $R_w = 0.2283$ (all reflections) and $R = 0.0740$ and $R_w = 0.2020$ [$I > 2\sigma(I)$]; those for **3c** are $R = 0.0689$ and $R_w = 0.1699$ (all reflections) and $R = 0.0566$ and $R_w = 0.1571$ [$I > 2\sigma(I)$]. Final R indices for **2e** are $R = 0.0992$ and $R_w = 0.2448$ (all reflections) and $R = 0.0636$ and $R_w = 0.1508$ [$I > 2\sigma(I)$]; those for **3e** are $R = 0.1235$ and $R_w = 0.2736$ (all reflections) and $R = 0.0674$ and $R_w = 0.1963$ [$I > 2\sigma(I)$]. The maximal residual peak and hole in the final difference electron density map are 257 and -382 e nm^{-3} for **2c**, 267 and -287 e nm^{-3} for **3c**, 182 and -191 e nm^{-3} for **2e**, and 270 and -380 e nm^{-3} for **3e**.

Full lists of atomic coordinates, bond lengths, angles, and thermal parameters have been deposited at the Cambridge Crystallographic Data Centre under deposition codes (**2c**) 205847, (**3c**) 205848, (**2e**) 205849, and (**3e**) 205850.

Experimental Determination of Partition Coefficient by Shake Flask Method. The solvents used were octanol and Sørensen buffer

(pH 7.4) mutually saturated with each other at room temperature. The two partitioning phases (w vs o) were used in ratios of 50:1 (compounds **2b,c**, **3b,c**, and **2e**, **2g,h**, **3g,h**), 25:1 (compound **2a**, **3a**), 10:2 (compound **3f**), 10:1 (compound **2f**, **3d,e**), 5:2 (compound **6**), and 1:1 (compounds **2d**, **4**, **5**, **7**). The starting amounts of the compounds were in the range of 2–20 mg dissolved in Sørensen buffer (50–220 mL), which was made from an aqueous 0.067 M $\text{Na}_2\text{HPO}_4 \cdot (2\text{H}_2\text{O})$ and from an aqueous solution of 0.067 M KH_2PO_4 . In the experiments the tubes were shaken mechanically in a shaking water bath for 1 h at 25 $^\circ\text{C}$ and then centrifuged for 10 min at 2000 rpm. The concentration of the compounds in the buffer was determined spectrophotometrically in 4–12 parallel measurements at the following wavelengths: 276 nm (compound **3d**), 284 nm (compound **7**), 291 nm (compound **3a**), 294 nm (compound **3e**), 296 nm (compounds **4–6**), 298 nm (compounds **3h**), 301 nm (compound **2a**), 304 nm (compounds **2d**, **3g**), 306 nm (compound **3f**), 318 nm (compound **3b**), 320 nm (compounds **3c**), 337 nm (compound **2b**), 338 nm (compounds **2c**), 340 nm (compound **2e,f**), 344 nm (compounds **2g**), and 348 nm (compounds **2h**).

Computational Methods. PM3 and DFT calculations were carried out by using the Spartan program package [Spartan SGI version 5.1.1, Wavefunction Inc., 1998, on a Silicon Graphics (INDY R4400) computer]. For calculation of Bird's indices (20) the optimized structures obtained at the PM3 level were used for full-geometry optimization with the LSDA/pBP86/DN/DFT model (21).

KOWWIN calculations were performed in two ways by using the KOWWIN program (version 1.54, Syracuse Research Corp., Syracuse, NY, 1997). [For an application, see: Meylan, W. M.; Howard, P. H. Atom/fragment contribution method for estimating octanol–water partition coefficient. *J. Pharm. Sci.* **1995**, *84*, 83–92.] A priori calculations were done by using the molecular structures or by operating with the EVA option, and predictions are made by considering the experimental log P value of one member of the series.

3DNET calculations (3DNET 4W, Version Beta 1.1.14, Vichem Chemie GmbH, Budapest, Hungary, 2001). [For an application, see: Kövesdi, I.; Dominguez-Rodriguez, M. F.; Orfi, L.; Náray-Szabó, G.; Varró, A.; Papp, G. J.; Mátyus, P. Application of neural networks in structure–activity relationships. *Med. Res. Rev.* **1999**, *19*, 249–269.] In the present study, geometric optimization for all 20 molecules was carried out by the MM2 program as implemented in HyperChem (HyperChem Professional, version 7.0 for Windows, Hypercube Inc., 2002) to obtain 3D structures. Then, for all molecules, 1437 structural descriptors were calculated with the Dragon program (version 2.1, by R. Todeschini, V. Consonni, and M. Pavan, 2002; available for download at <http://www.disat.unimib.it/chm/>). Of the descriptors, 1119 nonconstant ones were used in the subsequent computations. Next, contingency filtering with the XY linear correlation coefficient R^2 with the threshold of 0.4 yielded 423 descriptors for the subsequent variable subset selection. This large number of well-correlating descriptors indicated the possible existence of a good linear model. Therefore, a partial least-squares (PLS) analysis and quantitative structure–activity relationships (QSAR) model was built for the present study. In the Euclidean space of the 423 descriptors 6 uniformly distributed molecules were selected for external validation. With the remaining 14 molecules, a repeated evaluation ensemble method was used, in which 64 random selections of 7 molecules from 14 were generated. In each of these selections, 7 molecules were used to calculate the PLS model with a given number of components for a given subset of variables; the model was evaluated by the performance on the remaining set of 7 molecules. This process was repeated for all 64 random selections.

The ensemble average of the standard error of predictions over these 64 randomly selected evaluation sets was next chosen to be optimized during the variable subset selection. For each subset of variables, the number of PLS components was optimized to give the lowest ensemble-averaged standard error of predictions.

We used a genetic algorithm for the administrator of the variable subset selection, in which the negative of the ensemble-averaged standard error of predictions was taken as the fitness value of a given model. One hundred and thirty-nine generations of 16 models with 16 offspring resulted in the best model with 9 descriptors and 4 PLS components. This model was the best fitted one of the last 24 generations when the algorithm stopped. The final external validation

Table 1. Measured and Predicted $\log P$ and Calculated Dipole Moment (μ) Values of Compounds without and with a Nitro Group (**2a–c**, **3a–c**, and **4–6** and **2d–h** and **3d–h**, Respectively)

compd	$\log P_{\text{exptl}}$	$\log P_{\text{calcd}}$						μ (D) calcd
		KOWWIN	Δ	KOWWIN-EVA	Δ	3DNET	Δ	
2a	2.85	1.55	-1.30			2.78	-0.07	1.54
3a	1.87	0.80	-1.07	1.90 ^a	0.03	1.99	0.12	4.39
2b	3.02	1.76	-1.26	2.86 ^a	-0.16	2.94	-0.08	0.89
3b	2.10	1.01	-1.09	2.11 ^a	0.01	2.08	-0.02	4.31
2c	2.31	0.79	-1.52	2.41 ^b	0.01	2.59	0.28	1.80 ^f
3c	1.66	0.04	-1.62			1.68 ^e	0.02	3.31 ^f
4	0.66	-1.13	-1.79	0.49 ^b	-0.17	0.48	-0.18	1.86
6	-0.35	-1.88	-1.53	-0.26 ^b	0.09	0.00 ^e	-0.35	3.31
5	-0.34	-1.62	-1.28	0.00 ^b	0.34	0.17 ^e	0.51	1.86
7	-0.53	-2.37	-1.84	-0.75 ^b	-0.22	-0.57	-0.04	5.10
2d	1.71	-0.36	-2.07			1.40 ^e	-0.31	3.84
3d	0.76	-1.11	-1.87	0.96 ^c	0.20	0.83	0.07	1.97
2e	1.88	-0.14	-2.02	1.92 ^c	0.04	2.02	0.14	3.84 ^f
3e	1.25	-0.22	-1.47	1.17 ^c	-0.08	1.19	-0.06	3.37 ^f
2f	1.16	-1.12	-2.28	0.95 ^c	-0.21	1.22 ^e	0.06	4.58
3f	0.24	-1.87	-2.11	0.20 ^c	-0.04	0.41	0.17	4.27
2g	2.73	0.58	-2.15	2.64 ^d	-0.09	2.69	-0.04	4.53
3g	1.89	-0.17	-2.06			1.83	-0.06	2.28
2h	2.86	1.08	-1.78	3.13 ^d	0.27	2.65	-0.21	2.95
3h	2.46	0.33	-2.13	2.38 ^d	-0.08	2.28 ^e	-0.18	1.33

^a **2a** as reference. ^b **3c** as reference. ^c **2d** as reference. ^d **3g** as reference. ^e Result of the external validation. ^f Dipole moments calculated by using X-ray geometries are 1.67 (**2c**), 3.78 (**3c**), 5.11 (**2e**), and 1.66 (**3e**).

Table 2. Substituent Effect on the 3(2*H*)-Pyridazinone Ring

substituent	$\pi_X^a = \log P_{\text{RX}} - \log P_{\text{RH}}$		compounds compared
	π_X	π_{III} (22)	
-CH ₂ OH	-0.72	-1.03	2c vs 2b 3c vs 3b 2f vs 2e 3f vs 3e
-CH ₃	0.27	0.50	2e vs 2d 3e vs 3d 2b vs 2a 3b vs 3a
-NO ₂	0.33	-0.28	2g vs 2c 3g vs 3c
-CH ₂ -	0.35	0.50	2h vs 2g 3h vs 3g
-Cl	0.59	0.71	4 vs 5 6 vs 7
-C ₆ H ₅	1.61	1.96	2g vs 2f 3g vs 3f
-CH ₂ -C ₆ H ₅	1.83		2c vs 4 3c vs 6

^a π_X is a hydrophobic substituent constant.

of this model with the 6 molecules not used in the model generation process yielded an excellent $Q^2 = 0.915$ value, and the standard error of these predictions was as low as 0.292. After this procedure, a robust and demanding bootstrap type statistical test was performed to evaluate the predictive power of the model. In this process, the set of 20 molecules was randomly divided to a training set and a prediction set, each containing 10 molecules, and this was repeated 1024 times. The 9 descriptor/4 component PLS model was generated for each training set, and the Q^2 and the standard error of predictions were calculated for the corresponding prediction sets.

RESULTS AND DISCUSSION

The lipophilicities of 20 pyridazinone derivatives were expressed by $\log P_{\text{exptl}}$ values determined experimentally with

Table 3. Lipophilicity Difference of 3(2*H*)-Pyridazinone Regioisomers

pairs of regioisomers	$\Delta \log P = \log P_{4\text{-isomer}} - \log P_{5\text{-isomer}}$
	$\Delta \log P$
2a vs 3a	0.98
2b vs 3b	0.92
2c vs 3c	0.65
2d vs 3d	0.95
2e vs 3e	0.63
2f vs 3f	0.92
2g vs 3g	0.84
2h vs 3h	0.40
4 vs 6	1.01
5 vs 7	0.19

the standard shake flask method in an octanol–water system. The $\log P$ values were also calculated by two computer programs, KOWWIN, based on the AFC $\log P$ prediction method, and the 3DNET program using a neural network method.

Experimental $\log P$ Values. The $\log P_{\text{exptl}}$ values (**Table 1**) spanned a 3-order of magnitude wide lipophilicity range. In this series of compounds, the least lipophilic molecule was compound **7** ($\log P = -0.53$) and the most lipophilic one was **2b** ($\log P = 3.02$). Overall, the effect of substituents of the pyridazinone ring on lipophilicity followed the expected trend, and it could be understood by taking the standard π values into consideration (22). The average π values (π_X) of substituents on the pyridazinone ring are listed in **Table 2**. π_X is the hydrophobic substituent constant (by Hansch, Fujita) defined as the lipophilicity contribution of substituent X to lipophilicity of the molecule when replacing H by X.

The 4-amino isomers always had a higher lipophilicity than the corresponding 5-amino isomer with an average difference of 0.75 \log unit (**Table 3**). This finding is in agreement with our previous results (5) and confirms that not only the type but also the position of a substituent plays a significant role in the lipophilicity of the pyridazinone derivatives.

Structural Features of Regioisomers. The partition coefficient of a molecule is dependent on the electronic and steric

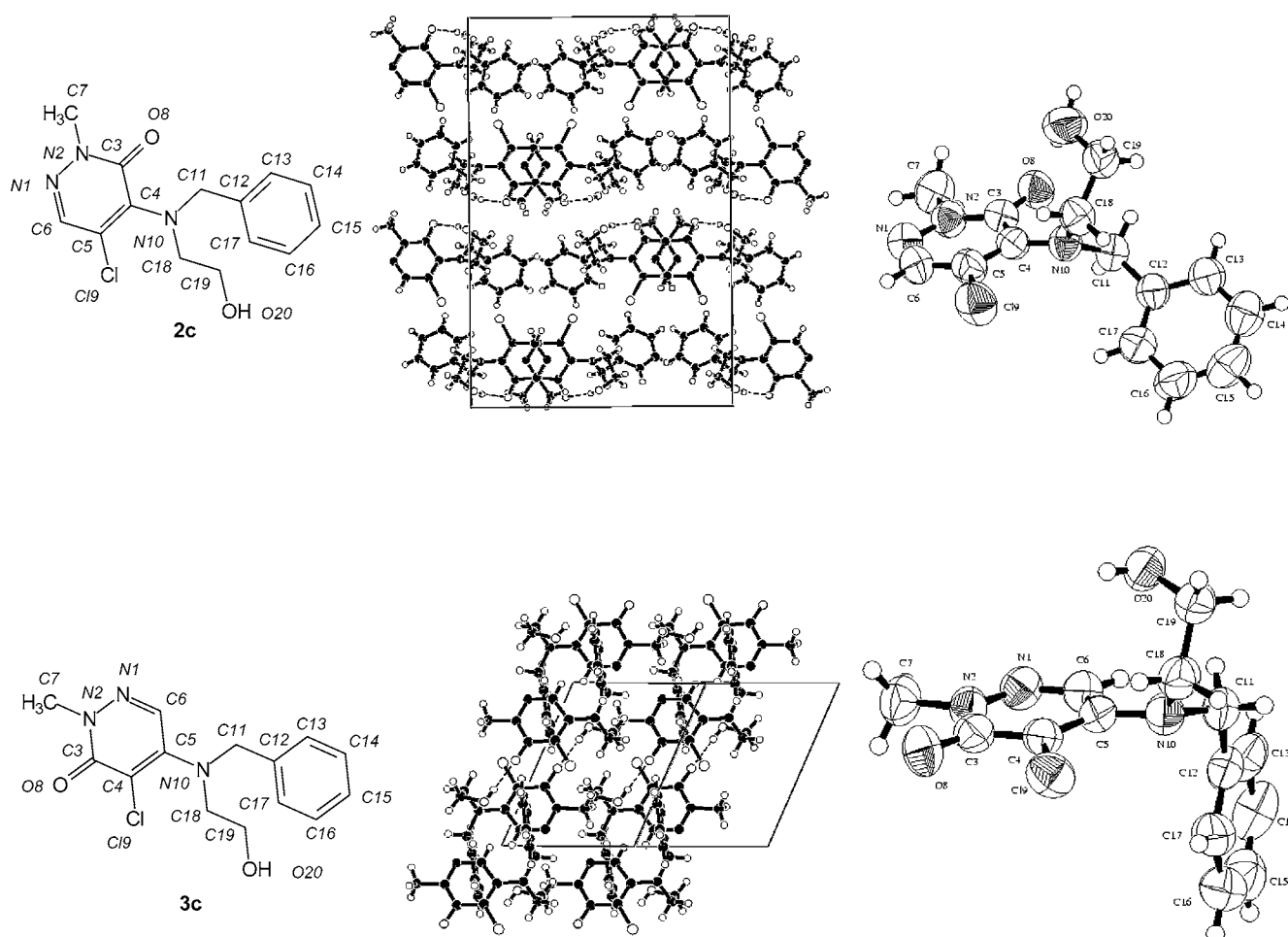


Figure 1. Elementary cells and ORTEP drawings with numbering of compounds **2c** and **3c**.

interactions within the structure. We focused first on the electronic properties, in particular, on the dipole moments of the 4- and 5-amino regioisomers. The dipole moment provides information on electronic distribution, and thereby it may also be related to the lipophilicity of compounds. Dipole moments were calculated by the semiempirical PM3 method as implemented in the Spartan package for both optimized and X-ray structures (Figures 1 and 2; Tables 4–6 of the Supporting Information), and the values are listed in Table 1 [μ (D) calcd, without and with superscript *f*, respectively]. Interestingly, in the first set of compounds possessing a hydrogen at the 6-position, dipole moments of 5-amino derivatives with lower log *P* values were found to be higher than those of the corresponding 4-amino compounds (cf. isomeric pairs of **2a–c** vs **3a–c**, **4** vs **6**, and **5** vs **7**). However, for the set of 6-nitro derivatives, the 4-amino compounds with higher log *P* values exhibited higher dipole moments than those of the 5-amino isomers (cf. **2d–h** vs **3d–h**). It is important to note that the negative pole of the dipole is the carbonyl group in the first set of compounds ($X = H$), whereas it is the nitro group in the second set ($X = NO_2$). Therefore, within this class of pyridazinones (which includes both sets of compounds), there exists no direct correlation between dipole moments and lipophilicity.

Next, X-ray structures of two pairs of regioisomers **2c**, **3c** and **2e**, **3e** (Figures 1 and 2, respectively) were carefully compared. The bond lengths (Tables 4–6, see Supporting Information), bond orders calculated with crystal and optimized geometries (Calc I, and Calc. II, respectively, in Table 7, see

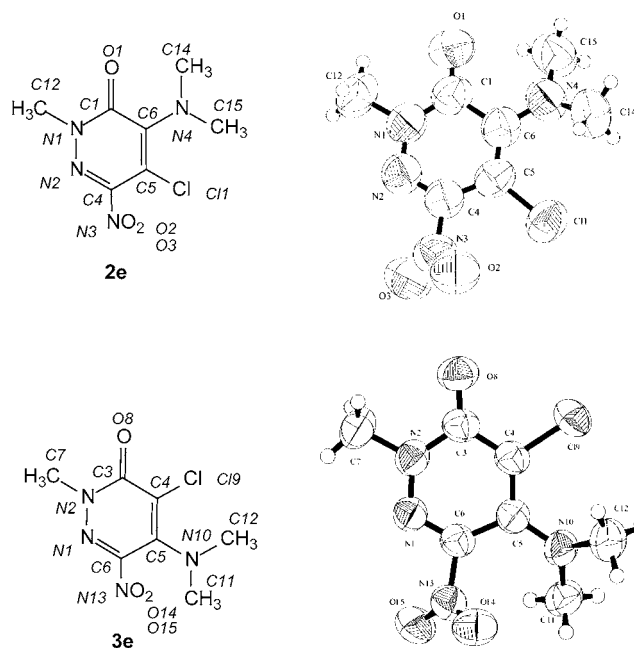


Figure 2. ORTEP drawings with numbering of compounds **2e** and **3e**.

Supporting Information), and H-bonding properties were considered. The X-ray structures of **2c** and **3c** reveal that the amine nitrogen atom (N10, for ORTEP numbering see Figure 1) is conjugated to the 3(2*H*)-pyridazinone moiety in both structures;

the angle of the 3(2*H*)-pyridazinone ring and the N10–C11–C18 plane is far from zero [52.9(2)° and 46.9(3)° for **2c** and **3c**, respectively]. The degree of conjugation is higher for **2c** as the bond connecting the amino group to the 3(2*H*)-pyridazinone ring is shorter and the configuration around N10 is closer to planar [distances of N10 from the plane of three adjacent carbon atoms is 0.0054(4) and 0.0263(3) nm for **2c**, and **3c**, respectively]. The steric crowding around N10 might result in higher *p*-character of its lone electron pair. Due to the opposite direction of conjugation in **2c** vs **3c**, in the former compound, the C3–C4 bond is significantly longer, whereas the C5–C6 bond is significantly shorter.

The corresponding torsion angles of the two regioisomeric compounds **2c**, **3c** are similar except for the ones defining the position of the benzyl group [–136.1(4)° for C4–N10–C11–C12 and –123.2(2)° for N10–C11–C12–C13 of **2c**; and –63.2(4)° for C5–N10–C11–C12 and 145.2(3)° for N10–C11–C12–C13 of **2c**], resulting in different overall shapes of the molecules with 42.03(1)° and 86.1(1)° for **2c** and **3c**, respectively, as the plane angles of the two aromatic moieties. The hydroxyl group in **2c** is also able to form an intramolecular hydrogen bond with the carbonyl oxygen in addition to the intermolecular one, whereas for **3c** there were detected only intermolecular hydrogen bridges. Nevertheless, conformations of the hydroxyethylene chains are very similar in both compounds.

The X-ray structures of **2e** and **3e** are shown in **Figure 2**, and the bond lengths and angles of the pyridazinone moiety are listed in Tables 5 and 6 of the Supporting Information (for ORTEP numbering see **Figure 2**). The amine nitrogen atom (i.e., N4 in **2e** and N10 in **3e**) was also found to be conjugated to the 3(2*H*)-pyridazinone ring in both structures. The degree of conjugation is much higher for **2e**, presumably due to the electron-withdrawing effect of the nitro group. Accordingly, in compound **2e**, the C1–C6 bond is longer, whereas the C6–C5 bond is shorter than the corresponding bonds in **3e**.

The steric interactions were considered. The higher lipophilicity of 4-amino regioisomers, particularly with a sterically demanding *N*-substituent, can be understood by taking the solvation into consideration. Increasing bulkiness around the pyridazinone carbonyl group, which may be the most important interaction site for the polar solvent (water) molecules during partition, would decrease water solubility and, accordingly, increase lipophilicity.

Considering all of the above data, it seems that values of single structural parameters such as bond lengths or bond orders are not necessarily translated into the differences of log *P* values. However, different intra- and intermolecular hydrogen bonding capacities as well as different solvation behavior of regioisomers appear to contribute to the observed trend of lipophilicity.

Calculated log *P* Values. The log *P* values were also determined by calculations (log *P*_{calcd}, **Table 1**). Two methods were applied on the basis of our previous promising experiences.

KOWWIN Program. The KOWWIN program was used in two operative ways. The a priori calculations were done by using the molecular structures. The log *P* values thus obtained differed very much (in several cases, >2 log unit errors were detected) from the experimentally determined log *P* data (**Table 1**, KOWWIN). Evidently, the program was able to reproduce neither the numerical values nor the trend of experimental log *P* values of the regioisomers. This finding illustrates how unreliable the prediction of log *P* data of new chemical structures can be. The KOWWIN program contains itself a solution to eliminate this deficiency. By operating with the EVA option,

predictions are made by correcting to the experimental log *P* value of one member of the series. On the basis of structural relationships, the log *P*_{exptl} value of one of the compounds **2a**, **3c**, **2d**, or **3g** was used as starting parameter; then the log *P* values of other compounds were calculated (log *P*_{calcd}). The results (**Table 1**, KOWWIN-EVA) were found to be dependent on the reference compound selected; nevertheless, these values were acceptable in terms of overall precision (the prediction was within the range of ±0.13 with the minimum of 0.01 and the maximum of 0.34 deviation).

Taking **2a** as reference, the average error of prediction was ±0.06 with minimum 0.01 and maximum 0.16 log unit deviations in the set of compounds **2b**, **3a,b** (**Table 1**, KOWWIN-EVA with superscript *a*). These acceptable results may be due to the fact that compounds **2b** and **3a,b** are structurally closely related to **2a**. All of these structures have a benzylamino group, and none of them has a nitro or hydroxy-alkyl group.

When **3c** was selected as reference structure for compounds **2c**, **4**, **5**, **6**, and **7**, the average error of the prediction was ±0.17 with minimum 0.01 and maximum 0.34 log unit deviations (**Table 1**, KOWWIN-EVA with superscript *b*). The higher deviation may be related to structural differences between the reference and test molecules: only the reference compound **3c** and, within the series tested, compound **2c** possess a benzyl group.

When compound **2d** was selected as reference structure, the program performed particularly well. The average error of prediction was ±0.12, with minimum 0.04 and maximum 0.21 log unit deviations for compounds **2e,f** and **3d–f** (**Table 1**, KOWWIN-EVA with superscript *c*), as a consequence of the structurally close relationship between reference and predicted structures.

With **3g** taken as reference compound, the average error of prediction was ±0.15 with minimum 0.08 and maximum 0.27 log unit deviations for molecules **2g,h** and **3h** (**Table 1**, KOWWIN-EVA with superscript *d*).

These results, together with our previous experiments with this program, indicate that the KOWWIN-EVA program with a carefully selected reference structure is able to reproduce experimental log *P* values of structurally closely related compounds.

3DNET Program. The 3DNET program incorporates a neural network analysis. The method is based on mathematical and statistical rules, and it is fully automated; as a consequence, there is no option for user intervention after the initial settings. In a recent study, it performed well on a large set of compounds: log *P* values were obtained with acceptable accuracy (10). The details of these calculations are described under Materials and Methods.

The best model of these calculations had acceptable parameters. The average *Q*² had a value of 0.857 for the predictions, and the value of average standard error of estimates was as low as 0.332. The standard deviations of these statistical parameters were 0.182 and 0.092, respectively. For the final model, nine structural descriptors could be identified. Their relative scores of importance computed on the full set of molecules are listed in Table 8 of the Supporting Information (23). One of the significant structural features found in this way to contribute to lipophilicity of regioisomers was the aromatic ratio. It is interesting to note that aromaticity of the regioisomers was found to differ by Bird's indices, too (for compounds **2d** and **3d** calculated values based on DFT-optimized geometries were 66 and 59, respectively).

In conclusion, lipophilicity of 4- and 5-amino-3(2*H*)-pyridazinones differs significantly; generally, the 4-amino derivatives have been found to possess higher log *P* values. It seems that hydrogen-bonding capacity and/or aromaticity are among the most relevant structural parameters that play important roles in the determination of log *P* values of this class of compounds. Moreover, the generally higher biological activity of the 4-aminopyridazinone regioisomers may be related to their significantly higher lipophilicity.

The calculated log *P* values obtained by KOWWIN-EVA and 3DNET computational methods were in good agreement with the experimental values. Nevertheless, our experiences with these programs suggest that a careful selection of the reference structure and the number of compounds included in the training set, respectively, may be of critical importance to reproduce experimental results.

ABBREVIATIONS USED

Log *P*, logarithm of partition coefficient; IR, infrared spectroscopy; FTIR, infrared spectroscopy with Fourier transformation; NMR, nuclear magnetic resonance spectroscopy; DEPT, ¹³C NMR spectroscopy with hydrogen decoupling and recorded in attached-proton test mode; mp, melting point; *R*_f, retention factor; *J*, coupling constant; μ , dipole moment; DFT, density functional theory; PLS, partial least-squares analysis; QSAR, quantitative structure–activity relationships; PM3, parametric method 3; π _X, hydrophobic substituent constant.

LIST OF COMPOUNDS

- 1a** 4,5-dichloro-2-methyl-3(2*H*)-pyridazinone
- 1b** 4,5-dichloro-2-methyl-6-nitro-3(2*H*)-pyridazinone
- 2a** 4-(*N*-benzylamino)-5-chloro-2-methyl-3(2*H*)-pyridazinone
- 2b** 4-(*N*-benzyl-*N*-methylamino)-5-chloro-2-methyl-3(2*H*)-pyridazinone
- 2c** 4-(*N*-benzyl-*N*-2-hydroxyethylamino)-5-chloro-2-methyl-3(2*H*)-pyridazinone
- 2d** 5-chloro-2-methyl-4-(methylamino)-6-nitro-3(2*H*)-pyridazinone
- 2e** 5-chloro-4-(dimethylamino)-2-methyl-6-nitro-3(2*H*)-pyridazinone
- 2f** 5-chloro-4-(*N*-2-hydroxyethyl-*N*-methylamino)-2-methyl-6-nitro-3(2*H*)-pyridazinone
- 2g** 4-(*N*-benzyl-*N*-2-hydroxyethylamino)-5-chloro-2-methyl-6-nitro-3(2*H*)-pyridazinone
- 2h** 4-(*N*-benzyl-*N*-3-hydroxypropylamino)-5-chloro-2-methyl-6-nitro-3(2*H*)-pyridazinone
- 3a** 5-(*N*-benzylamino)-4-chloro-2-methyl-3(2*H*)-pyridazinone
- 3b** 5-(*N*-benzyl-*N*-methylamino)-4-chloro-2-methyl-3(2*H*)-pyridazinone
- 3c** 5-(*N*-benzyl-*N*-2-hydroxyethylamino)-4-chloro-2-methyl-3(2*H*)-pyridazinone
- 3d** 4-chloro-2-methyl-5-(methylamino)-6-nitro-3(2*H*)-pyridazinone
- 3e** 4-chloro-5-(dimethylamino)-2-methyl-6-nitro-3(2*H*)-pyridazinone
- 3f** 4-chloro-5-(*N*-2-hydroxyethyl-*N*-methylamino)-2-methyl-6-nitro-3(2*H*)-pyridazinone
- 3g** 5-(*N*-benzyl-*N*-2-hydroxyethylamino)-4-chloro-2-methyl-6-nitro-3(2*H*)-pyridazinone

- 3h** 5-(*N*-benzyl-*N*-3-hydroxypropylamino)-4-chloro-2-methyl-5-nitro-3(2*H*)-pyridazinone
- 4** 5-chloro-4-(*N*-hydroxyethylamino)-2-methyl-3(2*H*)-pyridazinone
- 5** 4-(*N*-hydroxyethylamino)-2-methyl-3(2*H*)-pyridazinone
- 6** 4-chloro-5-(*N*-hydroxyethylamino)-2-methyl-3(2*H*)-pyridazinone
- 7** 5-(*N*-hydroxyethylamino)-2-methyl-3(2*H*)-pyridazinone

ACKNOWLEDGMENT

We are indebted to Á. Puhr for microanalyses and N. Bús for preparative assistance.

Supporting Information Available: Tables of bond lengths, bond angles, and bond orders of **2c**, **3c** and **2e**, **3e** and relative scores of nine descriptors. This material is available free of charge via the Internet at <http://pubs.acs.org>.

LITERATURE CITED

- (1) Kappe, T. Synthesis and chemistry of pyridazines functionalized in position 3 and 5 with heteroatoms. *J. Heterocycl. Chem.* **1998**, *35*, 1111–1122.
- (2) Mátyus, P.; Czákó, K.; Varga, I.; Jednakovics, A.; Papp Behr, Á.; Bódi, I.; Rabloczky, G.; Varró, A.; Jaszlits, L.; Miklós, A.; Lévy, L.; Schmidt, G.; Fekete, M.; Kürthy, M.; Szemerédi, K.; Zára, E. New 3(2*H*)-pyridazinone derivatives as antiarrhythmic agents. GB Patent 2262526; *Chem. Abstr.* **1994**, *120*, 77284.
- (3) Mátyus, P. 3(2*H*)-Pyridazinones: Some recent aspects of synthetic and medicinal chemistry. *J. Heterocycl. Chem.* **1998**, *35*, 1075–1089.
- (4) Károlyházy, L.; Freile, M.; Anwair, M. N. S.; Beke, Gy.; Giannini, F.; Castelli, M. V.; Sortino, M.; Ribas, J. C.; Zacchino, S.; Mátyus, P.; Enriz, R. D. Synthesis, *in vitro/in vivo* antifungal evaluation and structure–activity relationship study of 3(2*H*)-pyridazinones. *Arzneim.-Forsch.* **2003**, in press.
- (5) Károlyházy, L.; Szabó, D.; Anwair, M. A. S.; Borosy, A. P.; Takács-Novák, K.; Mátyus, P. Lipophilicity of regioisomers: A case study on 3(2*H*)-pyridazinones. *J. Mol. Struct. (THEOCHEM)* **2002**, *578*, 89–91.
- (6) Tsai, R.-S.; Carrupt, P.-A.; Testa, B.; El Tayar, N.; Grunewald, G. L.; Casey, A. F. Influence of stereochemical factors on the partition coefficient of diastereomers in a biphasic octan-1-ol/water system. *J. Chem. Res. (M)* **1993**, 1910–1920.
- (7) Van de Waterbeemd, H.; Mannhold, R. Lipophilicity descriptors for structure–property correlation studies: Overview of experimental and theoretical methods and a benchmark of log*P* calculations. In *Lipophilicity in Drug Action and Toxicology*; Pliska, V., Testa, B., Van de Waterbeemd, H., Eds.; In *Methods and Principles in Medicinal Chemistry*; Mannhold, R., Kubinyi, H., Timmerman, H., Eds.; VCH: Weinheim, Germany, 1996; Vol. 4, Chapter 23, pp 401–415.
- (8) Leo, A. The future of log*P* calculation. In *Lipophilicity in Drug Action and Toxicology*; Pliska, V., Testa, B., Van de Waterbeemd, H., Eds.; In *Methods and Principles in Medicinal Chemistry*; Mannhold, R., Kubinyi, H., Timmerman, H., Eds.; VCH: Weinheim, Germany, 1996; Vol. 4, Chapter 9, pp 157–171.
- (9) Van de Waterbeemd, H. Hydrophobicity of organic compounds: How to calculate it by personal computer. In *Booksoft Series*; Darvas, F., Ed.; Compudrug International: Vienna, Austria, 1986; Vol. 1.
- (10) Erös, D.; Kövesdi, I.; Örfi, L.; Takács-Novák, K.; Acsády, Gy.; Kéri, Gy. Reliability of log*P* predictions based on calculated molecular descriptors: A critical review. *Curr. Med. Chem.* **2002**, *9*, 1819–1829.

- (11) Duban, M. E.; Bures, M. G.; DeLazzer, J.; Martin, Y. C. Virtual screening of molecular properties: A comparison of log P calculators. In *Pharmacokinetic Optimization in Drug Research: Biological, Physicochemical and Computational Strategies*; Testa, B., Van de Waterbeemd, H., Folkers, G., Guy, R., Eds.; Wiley: New York, 2001; pp 485–497.
- (12) Dearden, J. C.; Bresnen, G. M. The measurement of partition coefficients. *Quant. Struct.–Act. Relat.* **1988**, *7*, 133–144.
- (13) Takács-Novák, K.; Józán, M.; Hermecz, I.; Szász, Gy. Lipophilicity of antibacterial fluoroquinolones. *Int. J. Pharm.* **1992**, *79*, 89–96.
- (14) Takács-Novák, K.; Józán, M.; Szász, Gy. Lipophilicity of amphoteric molecules expressed by the true partition coefficient. *Int. J. Pharm.* **1995**, *113*, 47–55.
- (15) Mowry, D. T. Mucochloric acid. II. Reactions of the aldehyde group. *J. Am. Chem. Soc.* **1953**, *75*, 1909–1912.
- (16) Tomio, T.; Azuma, H.; Hattori, R. 3-Methyl-4,5-dihalo-6-nitro-3(2H)-pyridazinone. Jpn. Patent 1300, 1967; *Chem. Abstr.* **1967**, *66*, 65497z.
- (17) Mátyus, P.; Czákó, K.; Behr, Á.; Varga, I.; Podányi, B.; von Arnim, M.; Várkonyi, P. Kinetic and theoretic aspects of regiochemistry in the reactions 4,5-dihalo-3(2H)-pyridazinones with benzylamines. *Heterocycles* **1993**, *36*, 785–798.
- (18) Éliás, O.; Károlyházy, L.; Stájer, G.; Fülöp, F.; Czákó, K.; Harmat, V.; Barabás, O.; Keserü, K.; Mátyus, P. Theoretical and experimental studies on ring closure reactions of 4(5)-chloro-5(4)-hydroxyalkylamino-6-nitro-3(2H)-pyridazinones. *J. Mol. Struct. (THEOCHEM)* **2001**, *545*, 75–96.
- (19) Matsuo, T.; Tsukamoto, Y.; Takagi, T.; Sato, M. Synthesis and biological activity of pyridazinoxazines. *Chem. Pharm. Bull.* **1982**, *30*, 832–842.
- (20) Bird, C. W. A new aromaticity index and its application to five-membered ring heterocycles. *Tetrahedron* **1985**, *41*, 1409–1414.
- (21) Hehre, W. J.; Lou, L. *A Guide to Density Functional Calculations in Spartan*; Wawefunction Inc.: Irvine, CA, 1997.
- (22) *Lipophilicity in Drug Action and Toxicology*; Pliska, V., Testa, B., Van de Waterbeemd, H., Eds.; In *Methods and Principles in Medicinal Chemistry*; Mannhold, R., Kubinyi, H., Timmerman, H., Eds.; VCH: Weinheim, Germany, 1996; Vol. 4.
- (23) Todeschini, R.; Consonni, V. Handbook of molecular descriptors. In *Methods and Principles in Medicinal Chemistry*; Mannhold, R., Kubinyi, H., Timmerman, H., Eds.; VCH: Weinheim, Germany, 2000; Vol. 11.

Received for review April 17, 2003. Revised manuscript received June 25, 2003. Accepted July 8, 2003. Financial support of this work by the National Research Foundation (T-31910) is acknowledged.

JF0343938